04.1;05.5

# Formation of the $Nb_3Sn$ phase by treating the Nb+Sn system with a pulsed electron beam

© Yu.N. Yurjev[1], A.V. Yurjeva[1], A.I. Saveljev[1], M.S. Vorobiev[2], P.V. Moskvin[2]

[1] Tomsk Polytechnic University, Tomsk, Russia
[2] Institute of High Current Electronics, Siberian Branch, Russian Academy of Sciences, Tomsk, Russia
E-mail: yurjev@tpu.ru

*Received September 27, 2023*
*Revised November 9, 2023*
*Accepted November 9, 2023*

The possibility of processing Nb−Sn films, which were deposited by magnetron sputtering, with a pulsed electron beam was investigated. Irradiation of coatings leads to the formation of the $Nb_3Sn$ phase. The films were irradiated with different beam energy densities and pulse durations. The surface morphology and phase composition of irradiated films were studied.

**Keywords:** Magnetron sputtering, $Nb_3Sn$ films, electron beam, plasma cathode, electron beam processing

DOI: 10.61011/PJTF.2024.03.57043.19741

The great interest in $Nb_3Sn$ films is due to the intensive development of accelerating equipment, and this compound has a higher critical temperature of transition to the superconducting state (18.3 K) [1,2] than pure Nb (9.2 K) or $V_3Ga$ (16.8 K). In this regard, triniobium stannide thin films can be used as coatings in superconducting radiofrequency resonators [3,4].

The purpose of the present work — to study the possibility of forming the $Nb_3Sn$ phase by electron-beam processing of films of the Nb−Sn system obtained by magnetron sputtering on copper substrates.

It is now known that films of $Nb_3Sn$ of the desired composition (19−26 at.% Sn) are successfully obtained by both physical and chemical methods [5,6]. Magnetron sputtering has such advantages as high sputtering speed (up to 10 $\mu$m/h), good adhesion of the deposited films and the ability to form films on substrates of different shapes and sizes. The use of a composite target is convenient from the point of view of composition control, since a change in the working pressure at constant power leads to a change in the ratio of atom sputtering fluxes, which affects the concentration of elements in the film [7]. In the present work, the deposition mode obtained previously is used [8].

To achieve the best superconductor properties, it is necessary to produce coatings with the highest content of the desired phase, large crystallites and few defects. Since the film often has an amorphous or fine-grained structure immediately after formation, it is common to carry out heat treatment to promote $Nb_3Sn$ phase formation and grain growth. Today, the main such method is vacuum annealing at high temperatures [9,10]. The disadvantages of this method are its energy consumption and the duration of the process.

Electron beam processing (EBP) of the coating [11,12] can serve as an alternative to vacuum annealing. The ability of the method to inject energy in batches into the coating provides heating of the surface layer to hundreds of thousands of degrees Kelvin, which can lead to the formation of the desired phase in less time. It is also possible to process the product with an electron beam and deposition of the coating in a single vacuum cycle [13,14].

The films were sputtered using a vacuum ion plasma system at an operating pressure of 0.3 Pa argon using a magnetron sputtering system at a power of 1 kW for 1 h. A disk composite target $Nb_3Sn$ was used as the sputtered material. A detailed description of the process of film preparation is presented in [8].

For EBP, a vacuum pulsed electron-beam „SOLO“ plant with an electron source with a plasma cathode based on a low-pressure arc discharge was used [15].

EBP of $Nb_3Sn$ films deposited on copper substrates was carried out from the coating side in argon atmosphere. The EBP scheme is given in Fig. 1.

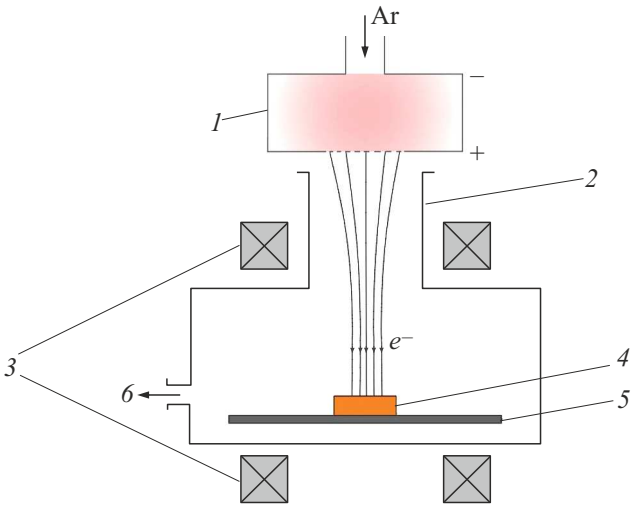


**Figure 1.** Electron Beam Processing Scheme. *1* — plasma cathode, *2* — drift tube, *3* — magnetic field coils, *4* — coated substrate, *5* — dual-axis manipulator, *6* — oil-free pumping.

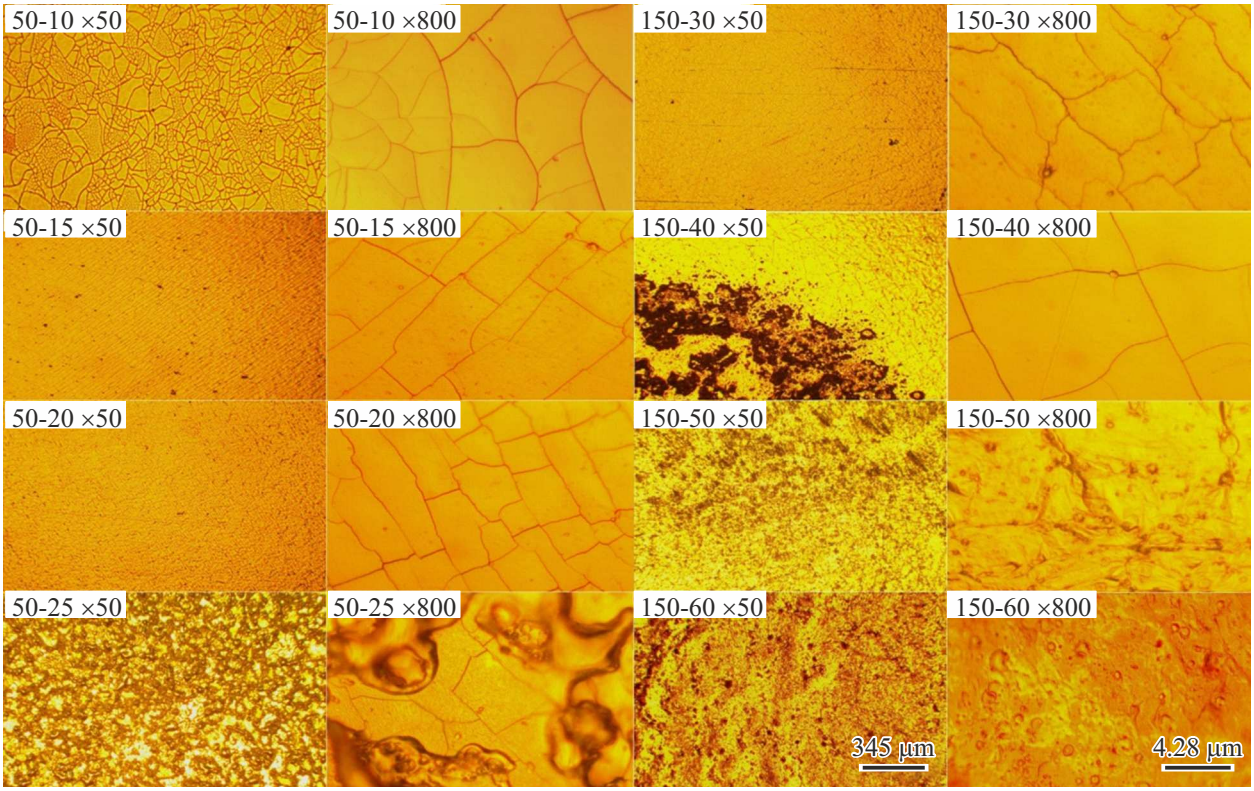


**Figure 2.** Photographs of the surface after processing at magnification ×50 and ×800.

**Table 1.** Elemental composition of the films $Nb_3Sn$

| Processing mode | Content, at.% | |
|---|---|---|
| | Nb | Sn |
| 50-10 | 77.98 | 22.02 |
| 50-15 | 77.11 | 22.89 |
| 50-20 | 77.35 | 22.65 |
| 50-25 | 81.45 | 18.55 |
| 150-30 | 77.09 | 22.91 |
| 150-40 | 83.62 | 16.38 |
| 150-50 | 89.24 | 10.76 |
| 150-60 | 88.97 | 11.03 |

Two EBP modes using beam durations of 50 and 150 $\mu$s were applied. The ranges of variation of the beam energy density were chosen for both modes: For 50 $\mu$s — 10–25 J/cm$^2$ in steps of 5 J/cm$^2$, for 150 $\mu$s — 30–60 J/cm$^2$ in steps of 10 J/cm$^2$. In each mode, three pulses of exposure with an interval of 3 s were performed. The processing modes are further denoted as follows: pulse duration ($\mu$s)-energy density (J/cm$^2$).

The surface of the samples before and after EBP was examined using an Altami MET 3C metallographic microscope at magnifications from ×50 to ×800. The phase composition of the samples was determined using a Shimadzu XRD-7000S diffractometer with Cu$K_\alpha$- radiation at an X-ray tube accelerating voltage of 40 kV and current of 30 mA. The angle step $\theta$ was 0.03° over the measurement range 2$\theta$ from 10 to 90°.

The images of $Nb_3Sn$ films after EBP are shown in Fig. 2. The samples irradiated at a pulse duration of 50 $\mu$s are characterized by the absence of melting zones, except for the 50-25 mode. In contrast, samples irradiated at a pulse duration of 150 $\mu$s are characterized by melting zones for all modes except mode 150-30.

Fig. 3 shows the radiographs of the coatings after EBP.

After electron beam processing, the films were examined by energy-dispersive spectroscopy using a Hitachi S-3400N electron microscope in order to study the elemental composition. The results obtained are shown in Table 1.

The Powder Cell program was used to determine the phase content. The study analyzed $Nb_3Sn$ and Cu. The results obtained are listed in Table 2.

After EBP of coatings at a pulse duration of 50 $\mu$s, the X-ray images show the presence of phases $Nb_3Sn$ and $Cu_3Sn$, as well as a peak corresponding to the copper substrate. The peak with the highest intensity corresponds to $Cu_3Sn$, indicating that mutual diffusion of copper substrate and tin from the coating has occurred. The coating irradiated in the 50-10 mode has minimal number of $Nb_3Sn$ peaks, which may indicate insufficient beam energy. The coating irradiated in the 50-25 mode also has few $Nb_3Sn$ peaks, which may be due to the insufficient tin content that has evaporated due to surface melting.

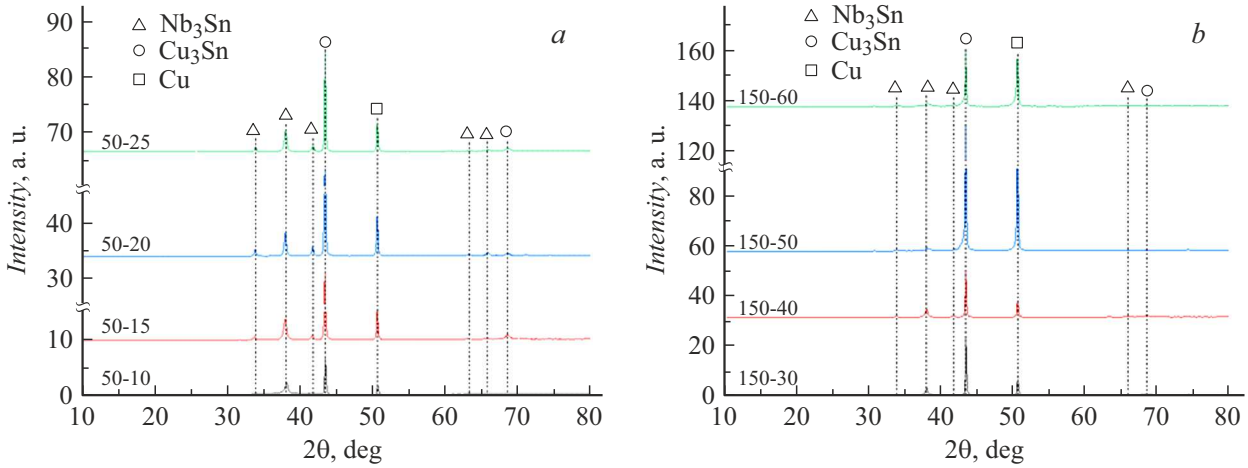


**Figure 3.** Radiographs of films irradiated at pulse durations of 50 (*a*) and 150 $\mu$s (b).

**Table 2.** X-Ray diffraction analysis of films $Nb_3Sn$

| Processing mode | Phase | Content, vol.% | Lattice constant, Å |
|---|---|---|---|
| 50-10 | $Nb_3Sn$<br>Cu | 15.8<br>84.2 | 5.2787<br>3.6023 |
| 50-15 | $Nb_3Sn$<br>Cu | 23.7<br>76.3 | 5.3092<br>3.6106 |
| 50-20 | $Nb_3Sn$<br>Cu | 26.8<br>73.2 | 5.3061<br>3.6123 |
| 50-25 | $Nb_3Sn$<br>Cu | 13.1<br>86.9 | 5.2939<br>3.6053 |
| 150-30 | $Nb_3Sn$<br>Cu | 18.2<br>81.8 | 5.2984<br>3.6060 |
| 150-40 | $Nb_3Sn$<br>Cu | 12.8<br>87.2 | 5.2947<br>3.6063 |
| 150-50 | $Nb_3Sn$<br>Cu | 4.6<br>95.4 | 5.2828<br>3.6082 |
| 150-60 | $Nb_3Sn$<br>Cu | 3.5<br>96.5 | 5.2896<br>3.6083 |

X-ray diffraction analysis of samples irradiated for 150 $\mu$s also showed the presence of peaks corresponding to $Nb_3Sn$, $Cu_3Sn$ and Cu. For all films, the reflex with the highest intensity corresponds to $Cu_3Sn$. The intensity of the $Nb_3Sn$ peaks is small because most of the Sn could diffuse from the film into the copper substrate and evaporate due to the strong heating that led to the melting of the coating. The largest peak $Nb_3Sn$ is observed for the film irradiated in the mode 150-30, which shows no signs of melting.

Thus, films of the Nb+Sn system were obtained by magnetron sputtering using a composite target. The formation of the $Nb_3Sn$ crystal structure was carried out by means of EBP of coating with a pulsed electron beam. Two modes of EBP of samples were used: with pulse durations of 50 and 150 $\mu$s and electron beam energy densities of 10–25 J/cm$^2$ for 50 $\mu$s and 30–60 J/cm$^2$ for 150 $\mu$s. Melting regions are observed for films processed at higher beam energy densities (modes 50-25, 150-40, 150-50, 150-60). Due to stronger heating and melting, there is intensive evaporation of tin from the film, leading to a decrease in the content of $Nb_3Sn$, which is confirmed by the data presented in Table 1. Films containing the maximum amount of $Nb_3Sn$ phase were obtained at EBP modes 50-15 and 50-20.

## Funding

This study was supported by the Russian Science Foundation (RSF grant № 21-12-00364).

### Conflict of interest

The authors declare that they have no conflict of interest.

## References

[1] M.N. Sayeed, U. Pudasaini, G.V. Eremeev, H.E. Elsayed-Ali, Vacuum, **212**, 112019 (2023). DOI: 10.1016/j.vacuum.2023.112019
[2] M.S. Shakel, M.N. Sayeed, G.V. Eremeev, A.-M. Valente-Feliciano, U. Pudasaini, H.E. Elsayed-Ali, Vacuum, **217**, 112563 (2023). DOI: 10.1016/j.vacuum.2023.112563
[3] N. Schäfer, N. Karabas, J.P. Palakkal, S. Petzold, M. Major, N. Pietralla, L. Alff, J. Appl. Phys., **128** (13), 133902 (2020). DOI: 10.1063/5.0015376
[4] C. Dong, Z. Lin, P. Sha, B. Liu, L. Ye, X. He, Physica C, **600**, 1354107 (2022). DOI: 10.1016/j.physc.2022.1354107
[5] M. Lu, F. Pan, H. Guo, S. Huang, Z. Yang, Q. Chu, F. Liu, A. Wu, T. Tan, Mater. Lett., **292**, 129557 (2021). DOI: 10.1016/j.matlet.2021.129557
[6] M.N. Sayeed, U. Pudasaini, C.E. Reece, G.V. Eremeev, H.E. Elsayed-Ali, J. Alloys Compd., **800**, 272 (2019). DOI: 10.1016/j.jallcom.2019.06.017
[7] M.N. Sayeed, U. Pudasaini, C.E. Reece, G.V. Eremeev, H.E. Elsayed-Ali, Appl. Surf. Sci., **541**, 148528 (2021). DOI: 10.1016/j.apsusc.2020.148528
[8] Yu.N. Yurjev, Yu.S. Bordulev, A.E. Kharisova, T.V. Selezneva, A.I. Savelev, A.I. Kazimirov, Russ. Phys. J., **65** (11), 1996 (2023). DOI: 10.1007/s11182-023-02861-z.
[9] E.A. Ilyina, G. Rosaz, J.B. Descarrega, W. Vollenberg, A.J.G. Lunt, F. Leaux, S. Calatroni, W. Venturini-Delsolaro, M. Taborelli, Supercond. Sci. Technol., **32** (3), 035002 (2019). DOI: 10.1088/1361-6668/aaf61f
[10] L. Xiao, X. Lu, Z. Yang, W. Tan, Y. Yang, L. Zhu, D. Xie, Physica C, **586**, 1353894 (2021). DOI: 10.1016/j.physc.2021.1353894
[11] M.S. Vorobyov, P.V. Moskvin, V.I. Shin, N.N. Koval, K.T. Ashurova, S.Yu. Doroshkevich, V.N. Devyatkov, M.S. Torba, V.A. Levanisov, Tech. Phys. Lett., **47**, 528 (2021). DOI: 10.1134/S1063785021050291.
[12] M. Vorobyov, T. Koval, V. Shin, P. Moskvin, M.K.A. Tran, N. Koval, K. Ashurova, S. Doroshkevich, M. Torba, IEEE Trans. Plasma Sci., **49** (9), 2550 (2021). DOI: 10.1109/TPS.2021.3089001
[13] V.N. Devyatkov, Y.F. Ivanov, O.V. Krysina, N.N. Koval, E.A. Petrikova, V.V. Shugurov, Vacuum, **143**, 464 (2017). DOI: 10.1016/j.vacuum.2017.04.016
[14] A.B. Markov, A.V. Mikov, G.E. Ozur, A.G. Padei, Instrum. Exp. Tech., **54** (6), 862 (2011). DOI: 10.1134/s0020441211050149
[15] V.N. Devyatkov, N.N. Koval, P.M. Schanin, V.P. Grigoryev, T.V. Koval, Laser Particle Beams, **21** (2), 243 (2003). DOI: 10.1017/S026303460321212X

*Translated by D.Kondaurov*